crystals

MDPI

Article

Preparation of Mixed Matrix Membranes Containing ZIF-8 and UiO-66 for Multicomponent Light Gas Separation

Eun Young Kim [1], Hyun Su Kim [1], Donghwi Kim [2], Jinsoo Kim [2] and Pyung Soo Lee [1,*]

[1] Department of Chemical Engineering and Material Science, Chung-Ang University, 84, Heukseok-ro, Dongjak-gu, Seoul 06974, Korea; dmsdud5766@daum.net (E.Y.K.); shfkstmzl@gmail.com (H.S.K.)
[2] Department of Chemical Engineering, Kyung Hee University, 1732 Deogyeong-daero, Giheung-gu, Yongin-si, Gyeonggi-do 17104, Korea; byein27@khu.ac.kr (D.K.); jkim21@khu.ac.kr (J.K.)
* Correspondence: leeps@cau.ac.kr; Tel.: +82-2-820-5939

Received: 26 November 2018; Accepted: 22 December 2018; Published: 26 December 2018

Abstract: Mixed matrix membranes (MMMs) containing zeolitic imidazolite framework-8 (ZIF-8) and UiO-66 as microporous fillers were prepared and evaluated their potential for the separation of a gas mixture produced by a methane reforming process. Hydrothermal synthesis was performed to prepare both the ZIF-8 and UiO-66 crystals, with crystal sizes ranging from 50 to 70 nm for ZIF-8 and from 200 to 300 nm for UiO-66. MMMs were prepared with 15% filler loading for both MMM (ZIF-8) and MMM (UiO-66). MMM (UiO-66) exhibited H_2 permeability of 64.4 barrer and H_2/CH_4 selectivity of 153.3 for single gas permeation, which are more than twice the values that were exhibited by a neat polymer membrane. MMM (ZIF-8) also showed better separation properties than that of a neat polymer membrane with H_2 permeability of 27.1 barrer and H_2/CH_4 selectivity of 123.2. When a gas mixture consisting of 78% Ar/18% H_2/4% CH_4 flowed into the membranes at 5 bar, the H_2 purity increased to as high as 93%. However, no improvement in the mixture gas separation performance was achieved by the MMMs as compared to that of a neat polymer membrane.

Keywords: mixed matrix membrane; metal oxide framework; gas separation; ZIF-8; UiO-66

1. Introduction

Reformation of carbonaceous gases, such as CO_2 and CH_4 [1], is considered a promising approach for addressing global warming problems. The products of the reforming processes can be valuable resources for energy generation and chemical production. Over the past few decades, various studies on catalyst design, reforming reaction engineering, and device development have been conducted to optimize certain reforming reactions. However, because both CO_2 and CH_4 are chemically stable, it is difficult to convert all feed gas into usable products during reformation [2]. In most commercially viable reforming reactions, only a fraction of CO_2 and CH_4 gases participate in the reactions, while the remainder do no react and instead form a mixture with the products. Therefore, a gas separation process must be performed to separate unreacted CO_2 and CH_4 from the reformate gases for further use.

While conventional gas separation processes [3], such cryogenic distillation, absorption, and adsorption, have been utilized for separation, membrane-based gas separation can be a strong alternative based on its low energy consumption and simple configuration [4]. Such features also lead to easy hybridization with existing reaction systems. A membrane separates gas mixtures that are based on permeability differences originating from diffusivity and solubility differences [5]. Based on the reforming reactions of CO_2 and CH_4, it is known that gases, such as hydrogen, ethylene, propane,

acetylene, and even large benzene can be produced. Such reformates have different physicochemical properties when compared to CH_4 and CO_2 gases, meaning that they can be separated by membrane processes based on diffusivity and solubility differences.

Currently, the main membrane materials utilized for gas separation are polymers. Membrane systems that are based on polymers have already been commercialized for many applications, including hydrogen recovery, natural gas treatment, and vapor recovery [6,7]. However, in a separation process where a large condensable gas is contained in the feed gas or large molecules are to be permeated through the membrane [8], the performance of polymer membranes is significantly degraded by swelling and the small fractional free volume of polymers. As mentioned above, because gas mixtures following the reformation of CO_2 and CH_4 contain large and condensable gases, polymer membranes have difficulty separating such gas mixtures, meaning that the development of novel membrane materials is required.

To overcome the limitations of polymer membranes, microporous membranes utilizing carbon molecular sieves, zeolite, and metal oxide frameworks (MOFs) film have been studied [9]. However, creating such membrane materials on a large scale is a challenging problem. In contrast, mixed matrix membranes (MMMs) can be easily scaled up and provide excellent separation performance and long-term operational stability as compared to polymer membranes [10]. An MMM is prepared by blending polymers with microporous material fillers, such as porous carbon, carbon nanotubes, zeolite, and MOFs [11–16]. Among the fillers for MMMs, MOFs have attracted significant attention based on their tunable pore structures and flexible frameworks, which have excellent compatibility with polymer matrices. The zeolitic imidazolite framework-8 (ZIF-8), a sub-family of MOFs, was mixed with polyimide and the resulting MMM was studied for various gas separation processes, including H_2/CO_2, CO_2/N_2, H_2/CH_4, and CO_2/C_3H_8 separation [17,18]. The synthesized MMMs exhibited higher gas permeability and selectivity when compared to a neat polyimide membrane and even showed molecular sieving characteristics at higher ZIF-8 loadings (>50% (w/w)). UiO-66 was also utilized as a filler and blended with polyimide, PIM-1, and polyether block amide for MMM fabrication [14,19,20]. High crystal dispersibility and CO_2 affinity were exhibited by the MMM containing amine-functionalized UiO-66. A cross-linkable co-polyimide/ZIF-8 MMM was prepared and tested for CO_2/CH_4 and propylene/propane separation [21,22]. The MMM was exhibited plasticization suppression based on the cross-linking reaction between the MOFs and polymer matrix.

Although there have been many studies on MMMs utilizing MOFs, most MMM studies have focused on CO_2 separation and MMM performance has been characterized by single gas permeation. Following carbonaceous gas reformation, the reformate mixture often contains three or more gases, including unreacted CO_2 and CH_4. Therefore, the separation performance of MMMs should be studied with multicomponent gas supplies. Based on this motivation, MMMs containing MOFs were synthesized, and their gas separation characteristics was studied for feed gases containing three gas components: H_2, Ar, and CH_4. ZIF-8, and UiO-66, which are mainly utilized in MMM research, were employed as fillers and a polyimide (Matrimid 5218®) with high intrinsic gas selectivity was utilized as a polymer matrix in this study.

2. Materials and Methods

2.1. Crystallization of ZIF-8 and UiO-66

ZIF-8 was prepared through a conventional solvothermal method [23], where 2-methylimidazole (304 mg, 8 mmol) and $Zn(NO_3)_2{\cdot}6H_2O$ (663 mg, 1 mmol) in 22.2 mL of methanol were mixed in a Teflon vessel and then reacted at 65 °C for 12 h. Following solvothermal synthesis, the products were purified via centrifugation and washed with methanol three times to remove any unreacted agents. Finally, the products were dried overnight in a 100 °C oven. UiO-66 was synthesized under typical reflux conditions. A mixture of zirconium(IV) oxychloride octahydrate (560 mg, 3.43 mmol) and 1,4-benzenedicarboxylic acid (380 mg, 3.43 mmol) in 20 mL of N,N-dimethylformamide (DMF)

was placed in a round vessel equipped with condenser and reacted at 120 °C for 24 h. Following synthesis, the products were purified via centrifugation and washed with DMF and ethanol to remove any unreacted agents. Finally, the products were dried overnight in a 100 °C oven.

2.2. Mixed Membrane Preparation

MMM films were prepared utilizing the solution-casting method. ZIF-8 and UiO-66 were dried at 100 °C under vacuum for 12 h, then added to N-methyl-2-pyrrolidone (NMP, BASF, Ludwigshafen, Germany), and sonicated for 120 min. Commercial polyimide (Matrimid 5218, Huntsman International LLC, Salt Lake City, UT, USA) was then dissolved in the NMP solution. The weight ratio of MOFs/polyimide in the NMP solutions was 15% (w/w). The solutions were stirred for 12 h at 60 °C, then sonicated for 60 min. The solutions were subsequently casted onto a glass plate under dry air flow and dried at 35 °C for 48 h. The casted films were then annealed at 180 °C in a vacuum oven for 24 h, after which they cooled naturally. The final thicknesses of membranes ranged from 40–60 μm, as measured by a digital micrometer.

2.3. Characterizations

Scanning electron microscopy (SEM) images were obtained by utilizing a Tescan Mira 3 LMU FEG with an acceleration voltage of 10 kV (TESCAN, Kohoutovice, Czech Republic). The samples were coated with platinum for 2 min in a Quorum Q 150T ES and their N_2 isotherm curves was measured at the temperature of liquid nitrogen (77 K) by utilizing a Micromeritics Tristar 3020 (Micromeritics, Norcross, GA, USA). Degassing was then performed at 423 K for 12 h under vacuum (~10^{-5} Torr) prior to N_2 sorption analysis. The specific surface areas of the samples were calculated utilizing the Brunauer-Emmett–Teller (BET) equation and their pore volumes were calculated to be $P/P_0 = 0.95$. Thermogravimetric analysis (TGA) was performed with a Sinco TGA-N 1000 (Sinco, Daejeon, Korea). Prior to TGA, the samples were kept in a chamber that was maintained at 80% relative humidity with an NH_4Cl salt solution for 12 h. Thermal analysis was conducted at a heating rate of 5 °C/min up to 700 °C under a constant flow of nitrogen (30 mL/min). The single gas permeability of the MMMs was measured based on the variable pressure method that was provided by Airrane Co. Ltd. (Daejeon, Korea). The membranes (9.6 cm^2) were mounted in a permeation cell and the permeation pressure on the permeate side was measured when it reached a steady state. The permeability coefficient (P, in cm^3 cm/cm^2 s cm Hg) was determined by

$$P = \frac{22414}{A} \times \frac{l}{\Delta p} \times \frac{V}{RT} \times \frac{dp}{dt} \quad (1)$$

where A is the membrane area (cm^2), l is the membrane thickness (cm), Δp is the pressure difference between the feed side and permeate side (psi), V is the permeate side volume (cm^3), R is the universal gas constant (6236.56 cm^3 cm Hg/mol K), T is the absolute temperature (K), and $\frac{dp}{dt}$ is the permeation rate (psi/s). The diffusion coefficient (D) was calculated using the time-lag method:

$$D = \frac{l^2}{6\theta} \quad (2)$$

where θ is the time-lag (s). The solubility coefficient, S, can be calculated using the following relationship:

$$P = D \times S \quad (3)$$

Finally, ideal gas selectivity was calculated by

$$\alpha\_ij = P\_i/P\_j = (D\_i/D\_j)(S\_i/S\_j) \quad (4)$$

where Pi and Pj are the gas permeabilities of gases i and j, respectively.

The gas flow system that is illustrated in Figure 1 was utilized to characterize mixed gas permeation performance of the MMMs. MMMs with effective membrane areas of 201 cm^2 were loaded into the permeation cell. The feed gas consisted of $H_2/CH_4/Ar$ and the permeate flow rate was altered by controlling the flow control meters on both the retentate side and permeate side. Feed pressure was set at 5 bar. A gas chromatograph (GC-2014, Shimadzu, Kyoto, Japan) was utilized to measure the concentrations of gases on the permeate side of the membranes.

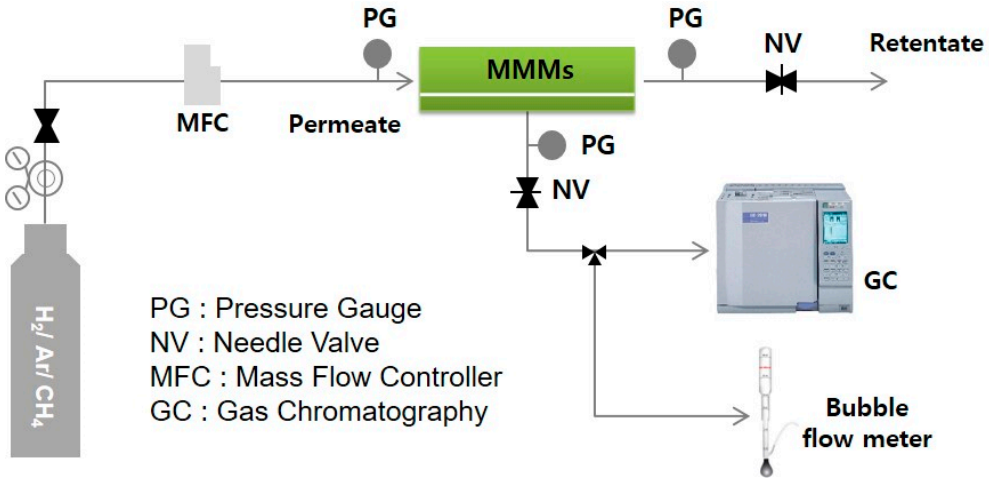

Figure 1. Gas flow system for measuring multicomponent gas separation through membranes.

3. Results and Discussion

3.1. Characterization of ZIF-8 and UiO-66

The morphologies and crystal structures of the synthesized ZIF-8 and UiO-66 crystals were confirmed via SEM, X-ray diffraction (XRD, Rigaku, Tokyo, Japan), and nitrogen isotherms. The results are presented in Figure 2. As shown in Figure 2a, the particle size of the ZIF-8 was 50–70 nm. The XRD of the samples shown in Figure 2b indicated pure-phase ZIF-8 crystals with no other crystalline structures. Slight peak broadening was observed in the XRD results because of the small crystal size. The nitrogen isotherm of ZIF-8 was a type I isotherm, as shown in Figure 2c. The first volume uptake of nitrogen at very low pressures indicates the presence of micropores and the second adsorption of nitrogen beginning at a relative pressure of 0.8 was likely caused by mesopores generated by the packing of nanocrystals. The texture properties of ZIF-8 showed a BET surface area of 1630 m^2/g and total pore volume of 1.08 cm^3/g, similar to the values that are reported in the literature [24]. The crystal size of UiO-66 was 200–400 nm, as shown in Figure 2d, which is larger than the ZIF-8 crystals. One can see from Figure 2e that the XRD of UiO-66 revealed a pure crystalline phase of the UiO-66 framework, where the peak was a bit shaper than that of the ZIF-8 because of the larger crystal size. The nitrogen isotherm of UiO-66 was also a type I isotherm, as shown in Figure 2f, but the second nitrogen adsorption was smaller when compared to that of ZIF-8. The BET surface area of the UiO-66 was calculated to be 1317 m^2/g and the total pore volume was 1.57 cm^3/g, which are also similar to the values in the literature [25].

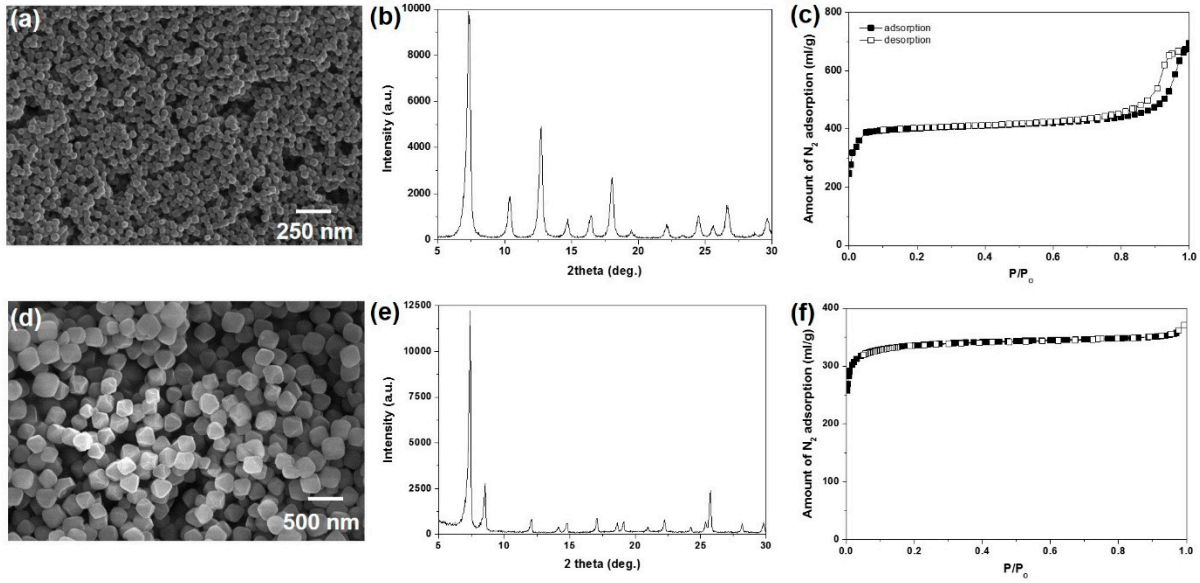

Figure 2. Physical properties of synthesized zeolitic imidazolite framework-8 (ZIF-8) and UiO-66 crystals. (**a**) Scanning electron microscopy (SEM) image; (**b**) X-ray diffraction (XRD); and (**c**) nitrogen isotherm of ZIF-8 and (**d**) SEM image; (**e**) XRD; and (**f**) nitrogen isotherm of UiO-66.

3.2. Characterization of Membranes

The MMMs were prepared utilizing the synthesized ZIF-8 and UiO-66 with loadings of 15%. By considering film processability and physical flexibility, filler loading of 15% was selected for both MMM (ZIF-8) and MMM (UiO-66), though more fillers could be incorporated into the polyimide. As described elsewhere, MMM with higher filler loading exhibited improved gas permeability. However, the membrane was less reproducible and slightly fragile. Furthermore, a large membrane area (>15 cm^2 in diameter) was required to obtain detectable gas flux both by GC and using gas flow meter in this study. Therefore, MMM with 15% filler loading was chosen, which was reproducible and physically stable. Figure 3 presents SEM images of MMM (ZIF-8) and MMM (UiO-66). The average thickness of the MMMs was 40–60 μm, as shown in Figure 3b,d. Our membranes were flexible and they did not break when folded in half. Dried powders of both ZIF-8 and UiO-66 were dispersed into NMP solutions for MMM preparation. Several previous articles reported that MOF particles were not redispersible at higher loadings, leading to the formation of grape-like morphologies [26]. However, as shown in Figure 3, after the dispersion of particles into solvent by assist of sonication, both fillers were well dispersed into the polymer matrix at a loading of 15% in this study. Even the ZIF-8 filler, whose average crystal size was less than 70 nm, exhibited uniform dispersion into the polymer matrix, as shown in Figure 3a. As an example, when ZIF-8 filler with particles of < 50 nm was employed, the dispersion of ZIF-8 powder was poor. Furthermore, defects originating from poor interactions between the polymer and fillers were not observed in either sample, as shown in the insets in Figure 3b,d, which reflects desirable MOF and polymer interactions, as reported in previous articles [27]. Thus, it is thought that both MMMs were successfully prepared from our approach.

The thermal stability of all samples, namely ZIF-8, UiO-66, the neat polymer film, MMM (ZIF-8), and MMM (UiO-66), was further analyzed via TGA, as shown in Figure 4. As shown in Figure 4a, The ZIF-8 powder showed small loss below 200 °C, because of trapped gases and solvents. This weight loss plateaued at 400 °C. Decomposition of the ZIF-8 occurred at approximately 400 °C and only 25% of the material remained following the TGA measurements. The UiO-66 showed weight loss in the range of 25–200 °C because of trapped molecules, but the amount was much larger than that of ZIF-8. Additional weight loss occurred in the range of 200–300 °C as a result of the dihydroxylation of $Zr_6O_4(OH)_4$ into Zr_6O_6. Gradually, weight loss also continued after 500 °C based on the removal of benzene moiety in the UiO-66 framework. In the case of the polymer film, no noticeable weight loss

occurred below 450 °C, after which polymer deposition began to decompose. Over the temperature range 500–700 °C, continuous weight loss was observed due to the degradation of the polymer, followed by evaporation of light gases, like hydrogen, carbon dioxide, and methane from the polymer backbone [28]. Thermal decomposition features associated with MOFs and polymer films appeared in the TGA results for MMM (ZIF-8) and MMM (UiO-66), as shown in Figure 4. In the case of MMM (UiO-66), the first weight loss temperature originated from polymer chain decompositions that occurred at lower temperatures when compared to that in the neat polymer film shown in Figure 4b. These results indicate that favorable interactions between the Matrimid 5218® and UiO-66 enhanced the thermal stability of the membranes, which matches observations in the literature [29]. However, the favorable interaction was not clearly revealed with MMM (ZIF-8), because decomposition of ZIF-8 started first and overlapped with the temperature of polymer film decomposition.

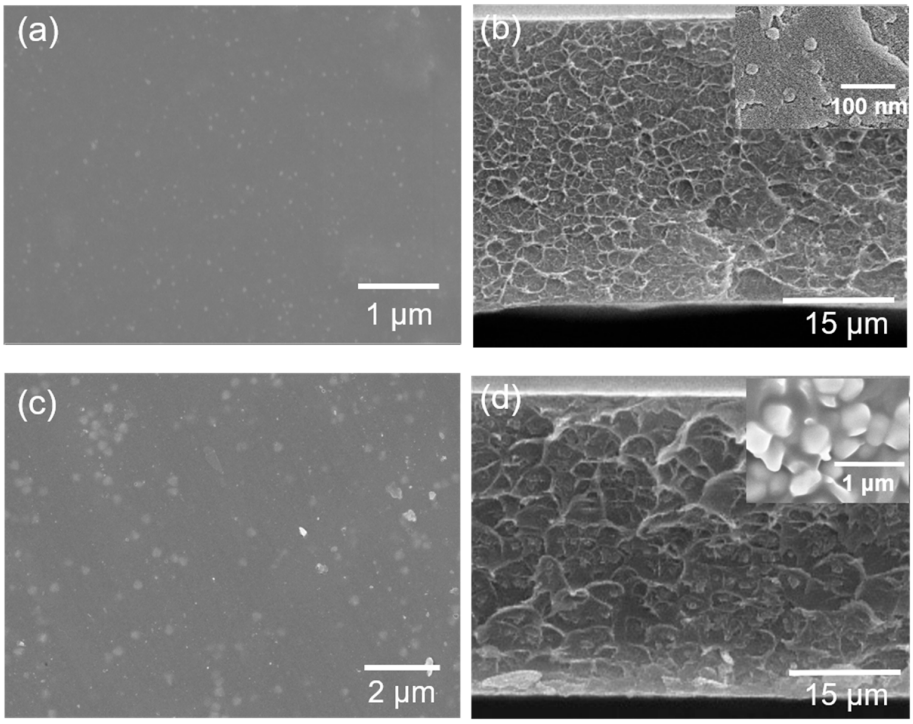

Figure 3. SEM images of mixed matrix membranes (MMMs). (**a**) Top view of MMM (ZIF-8); (**b**) cross-sectional view of MMM (ZIF-8); (**c**) top view of MMM (UiO-66); and (**d**) cross-sectional view of MMM (UiO-66).

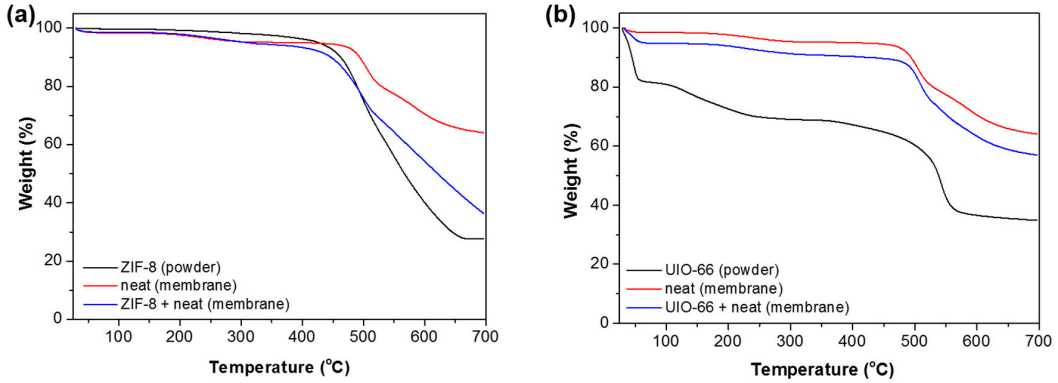

Figure 4. Thermogravimetric analysis (TGA) of ZIF-8, UiO-66, polyimide, MMM (UiO-66), and MMM (ZIF-8). (**a**) TGA of ZIF-8, polyimide, and MMM (ZIF-8) and (**b**) TGA of UiO-66, polyimide, and MMM (UiO-66).

3.3. Single Gas Permeation Through Membranes

Figure 5 presents the single gas permeation results for membranes that were prepared from pure polyimide and MMMs with 15% loadings of ZIF-8 and UiO-66. As shown in Figure 5a, gas permeability decreased as the kinetic diameter of the gas increased for all membranes, following typical trends for gas separation membranes. Figure 5a,b clearly demonstrate that the presence of MOFs in the polymer matrix led to improvements in both gas permeability and ideal gas selectivity for H_2/CH_4, CO_2/CH_4, and Ar/CH_4. These increases in gas permeability and ideal gas selectivity indicate that the MMMs were successfully prepared without defects and that ZIF-8 and UiO-66 are effective fillers for MMMs, as suggested in the literature. The gas permeability of MMM (UiO-66) was greater than that of ZIF-8 for all gas flow tests, because the window diameter of UiO-66 ($\varphi \sim 0.60$ nm) is larger than the pore aperture of ZIF-8 ($\varphi \sim 0.34$ nm). Gas permeation was further analyzed by calculating the diffusion and solubility coefficients of penetration, which are listed in Table 1. Interestingly, the gas permeability of MMM (ZIF-8) for N_2 and CH_4 is greater than that of polyimide, even though the pore aperture size of ZIF-8 is approximately 0.34 nm, which is impermeable for N_2 and CH_4. As shown in Table 1, the solubility of both N_2 and CH_4 for MMM (ZIF-8) was greatly increased as compared to that for polyimide. Therefore, it seems that the flexible structure of ZIF-8, referred to as the "gate-opening" effect [30], rather than defects in the separation membrane, contributes to increased permeability for N_2 and CH_4. Additionally, the gas permeability of MMM (UiO-66) was greater than that of MMM (ZIF-8). This increase originated not from diffusivity, but from solubility, despite the larger pores of MMM (UiO-66). It is postulated that the existence of linker vacancies in the UiO-66 framework may enhance adsorption of gas molecule, leading to improved solubility of gas molecules in MMM (UiO-66) [31].

Table 1. Solubility and diffusivity of membranes.

Sample	Gases	Diffusivity (cm^2/s)	Solubility ($cm^3(STP)/cm^3cmHg$)	Permeability (barrer)
PI	H_2	N.D. *	N.D. *	11.7
	CO_2	8.22×10^{-9}	6.24×10^{8}	5.1
	Ar	2.83×10^{-8}	1.28×10^{7}	0.36
	N_2	8.97×10^{-9}	1.58×10^{7}	0.14
	CH_4	2.81×10^{-9}	5.04×10^{7}	0.14
MMM(UiO-66(15%))	H_2	N.D. *	N.D. *	64.4
	CO_2	7.10×10^{-9}	3.81×10^{9}	27.1
	Ar	1.51×10^{-7}	9.01×10^{6}	1.4
	N_2	6.92×10^{-9}	7.40×10^{7}	0.51
	CH_4	1.25×10^{-9}	3.32×10^{8}	0.42
MMM(ZIF-8(15%))	H_2	N.D. *	N.D. *	27.1
	CO_2	8.02×10^{-9}	1.16×10^{9}	9.3
	Ar	1.13×10^{-8}	5.31×10^{7}	0.60
	N_2	6.68×10^{-9}	3.34×10^{7}	0.22
	CH_4	1.66×10^{-9}	1.33×10^{8}	0.22

* N.D.: Not Determined. Hydrogen permeated though membranes too fast to calculate time-lag.

The Robson plots of MMM (UiO-66) and MMM (ZIF-8) for CO_2/CH_4 and H_2/CH_4 separation (Figure 6) show that the membranes designed herein exhibited comparable performance with reported mixed matrix membranes. However, our membranes did not exceed the upper bound of polymeric membranes (2008), possibly due to relatively low filler loading (15%) [32].

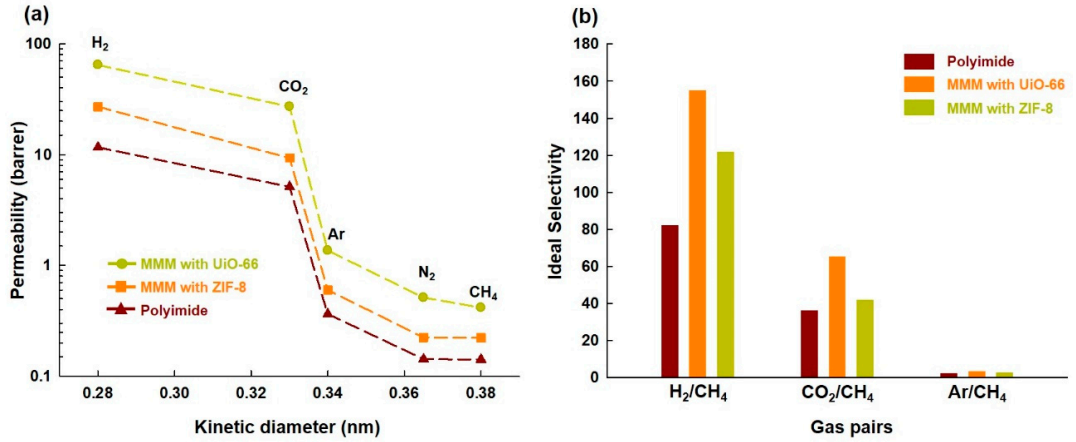

Figure 5. Single gas permeation of polyimide, MMM (UiO-66), and MMM (ZIF-8). (**a**) Single gas permeability of gas molecules and (**b**) ideal gas selectivity.

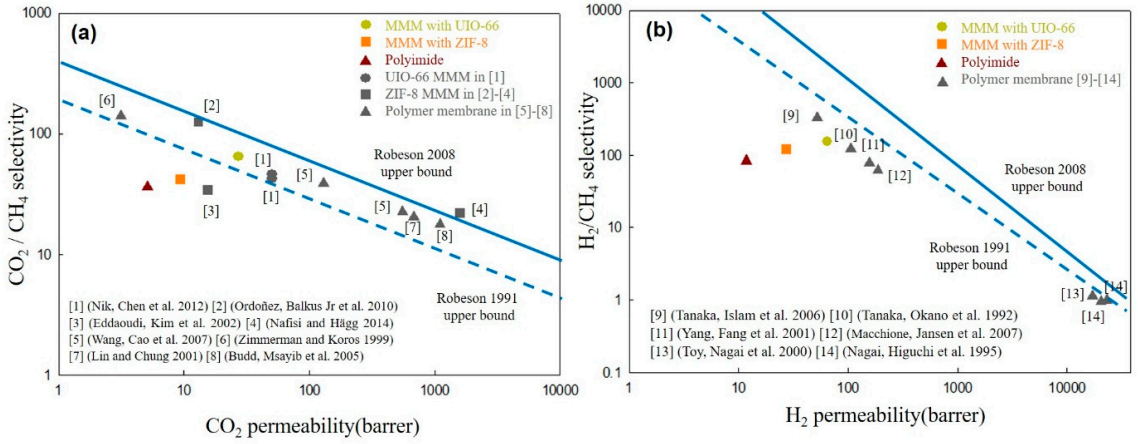

Figure 6. Upper bound of membranes for gas separation. (**a**) CO_2/CH_4 and (**b**) H_2/CH_4 separations.

3.4. Multiple Gas Mixture Permeations Through MMMs

One can see from Figure 5 that the MMMs have superior gas separation properties when compared to a pure polymer membrane. Therefore, the MMMs were applied to separate multiple gas mixtures that were produced by a methane reforming reaction. Figure 7a depicts a methane reforming process and subsequent separation process [33]. This process reforms methane via Ar plasma reaction into hydrocarbons, such as ethane and acetylene. Following the reaction, several components are present in the product stream, including hydrogen and hydrocarbon as products, along with unreacted argon and methane. Hydrocarbons from the gas mixture can be easily recovered via pressure swing adsorption or distillation processes, after which hydrogen, argon, and methane remain. When membrane separation is utilized, it may be possible to simultaneously purify hydrogen and recycle argon and methane from the initial plasma reaction, as shown in Figure 7a. Based on this concept, the separation performances of the MMMs were tested at 5 bar with a mixed gas flow (78% Ar, 4% CH_4, and 18% H_2) selected from one of the methane reforming reactions. The gas compositions on the permeate side were characterized via gas chromatography. The results are presented in Figure 7b. As shown in Figure 7b, the hydrogen concentration significantly increased following membrane separation for all membrane materials. However, when compared to the polyimide membranes, the MMMs showed no advantages in terms of mixed gas separation performance. In fact, the polyimide membrane was better at separating hydrogen from argon and methane compared to the MMMs, which is inconsistent with previous single gas measurement data. Furthermore, the performance of MMM (UiO-66) was the lowest overall, despite showing the best results for single gas permeation. This experiment repeated more than

10 times by changing membranes and tuning parameters to check for possible errors in measurement or membrane preparation. All of the data followed a similar trend. Therefore, it is postulated that the interactions between diffusing molecules must have affected the separation dynamics of the membrane and eventually affected separation performance.

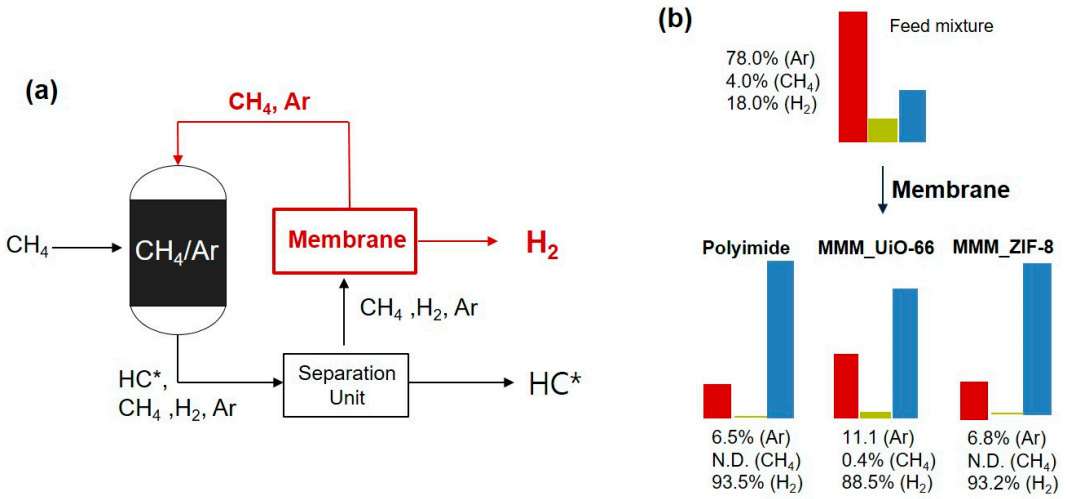

Figure 7. Multicomponent mixture gas separation system. (**a**) Conceptual hybrid system with methane reforming reaction and membrane-based gas separation; (**b**) Mixed gas separation properties of polyimide, MMM (UiO-66), and MMM (ZIF-8). * HC: hydrocarbon.

Additional research to understand changes in membrane performance based on the composition of mixed gases is underway by tuning operation parameters, such as pressure, temperature, and stage-cuts.

As shown in Table 2, both gas permeability and selectivity under mixture gas flow were lower than those for a single gas. To obtain sufficient gas flux for characterization of gas permeate composition by GC, 5 bar of feed pressure was applied, which is much higher than that required for single gas measurement. As for the "dual sorption model", total gas sorption into a membrane is decreased with increasing feed pressure because "Langmuir Sorption" becomes saturated at high pressures [34,35]. Thus, the decrease in sorption may result in some corresponding decrease in gas permeance of H_2, Ar, and CH_4. However, each gas exhibited a different degree of reduction in gas permeance. The reduction for CH_4 was less than those for the other two. The critical temperature for CH_4 (190.6 K) is higher than those for H_2 (33.2 K) and Ar (158 K), reflecting that CH_4 sorption is greater than H_2 and Ar sorption [35]. Thus, strong sorption of CH_4 on polymer should competitively reduce the sorption of H_2 and Ar, leading to further reductions in H_2 and Ar permeabilities. The bulkier methane gas adsorbed in micropores of MOF fillers could also slow down the diffusion of H_2 and Ar through MMMs. However, the extent of reduction in permeance for each gas also depended on the type of membrane. It is thought that the difference is originated from the frameworks of fillers. Further research is underway to understand changes in the membrane performance in terms of membrane materials.

Table 2. Mixture gas permeability and selectivity.

Membrane	Mixture Gas Permeability (barrer)			Mixture Gas Selectivity			Ideal Gas Selectivity		
	H_2	Ar	CH_4	H_2/CH_4	H_2/Ar	Ar/CH_4	H_2/CH_4	H_2/Ar	Ar/CH_4
PI	9.1 (−22%)	0.15 (−58%)	N.D. *	-	62.3	-	85.7	32.5	2.6
MMM (UiO-66)	18.3 (−72%)	0.52 (−63%)	0.37 (−12%)	49.2	34.9	1.4	153.3	46.0	3.3
MMM (ZIF-8)	14.5 (−46%)	0.24 (−60%)	N.D. *	-	59.4	-	123.2	45.2	2.7

* N.D.: Not Determined. Methane concentration was below the detection limit of GC. Numbers inside parentheses indicated percent changes of gas permeability, with respect to single-gas permeation measurements by the time-lag method.

4. Conclusions

MMMs, including MOFs as fillers, were prepared to study membrane-based multicomponent gas separation of the products of methane reforming reactions. ZIF-8 and UiO-66 were prepared for the MMMs and exhibited well-developed crystalline structures with monodisperse crystal size distributions based on XRD, SEM, and nitrogen isotherm analysis. Based on desirable interactions between MOFs, polyimide, and NMP, individual MOF crystals were uniformly dispersed over a polymer matrix; no large clusters or aggregates were observed by SEM. MMM (UiO-66) exhibited a higher gas flux and gas selectivity based on single gas permeation measurements than those of a pure polymer film, MMM (ZIF-8), and MMM (UiO-66). However, when a mixed gas containing $H_2/Ar/CH_4$ was separated by the membranes, no major differences were observed in the separation performance. This result was very different from the single gas permeation result, which indicates that there were multiple diffusant-diffusant and diffusant-molecule interactions. An MMM may provide a very complex gas diffusion route, because both solution diffusion and surface pore diffusion may occur simultaneously when the membrane is in use. An in-depth study of multicomponent separation via MMM is essential for their commercialization.

Author Contributions: P.S.L. performed the initial experiments and conceived the project. E.Y.K. and H.S.K. contributed to MMM preparation and characterization. D.K. and J.K. prepared MOFs. P.S.L. and E.Y.K. prepared the manuscript. P.S.L. and J.K. directed all aspects of the project.

Funding: This research was fundeded by the Chung-Ang University Research Grants in 2018, and also supported by National Research Foundation of Korea (Grant number: NRF-2018R1D1A1B07049245).

Conflicts of Interest: The authors declare no conflicts of interest.

References

1. Wang, S.; Lu, G.; Millar, G.J. Carbon dioxide reforming of methane to produce synthesis gas over metal-supported catalysts: State of the art. *Energy Fuels* **1996**, *10*, 896–904. [CrossRef]
2. York, A.P.; Xiao, T.; Green, M.L. Brief overview of the partial oxidation of methane to synthesis gas. *Top. Catal.* **2003**, *22*, 345–358. [CrossRef]
3. Leung, D.Y.; Caramanna, G.; Maroto-Valer, M.M. An overview of current status of carbon dioxide capture and storage technologies. *Renew. Sustain. Energy Rev.* **2014**, *39*, 426–443. [CrossRef]
4. Bernardo, P.; Drioli, E.; Golemme, G. Membrane gas separation: A review/state of the art. *Ind. Eng. Chem. Res.* **2009**, *48*, 4638–4663. [CrossRef]
5. Baker, R.W.; Low, B.T. Gas separation membrane materials: A perspective. *Macromolecules* **2014**, *47*, 6999–7013. [CrossRef]
6. Yang, H.; Xu, Z.; Fan, M.; Gupta, R.; Slimane, R.B.; Bland, A.E.; Wright, I. Progress in carbon dioxide separation and capture: A review. *J. Environ. Sci.* **2008**, *20*, 14–27. [CrossRef]
7. Galizia, M.; Chi, W.S.; Smith, Z.P.; Merkel, T.C.; Baker, R.W.; Freeman, B.D. 50th anniversary perspective: Polymers and mixed matrix membranes for gas and vapor separation: A review and prospective opportunities. *Macromolecules* **2017**, *50*, 7809–7843. [CrossRef]
8. Vu, D.Q.; Koros, W.J.; Miller, S.J. Effect of condensable impurity in CO_2/CH_4 gas feeds on performance of mixed matrix membranes using carbon molecular sieves. *J. Membr. Sci.* **2003**, *221*, 233–239. [CrossRef]
9. Goh, P.; Ismail, A.; Sanip, S.; Ng, B.; Aziz, M. Recent advances of inorganic fillers in mixed matrix membrane for gas separation. *Sep. Purif. Technol.* **2011**, *81*, 243–264. [CrossRef]
10. Chuah, C.Y.; Goh, K.; Yang, Y.; Gong, H.; Li, W.; Karahan, H.E.; Guiver, M.D.; Wang, R.; Bae, T.H. Harnessing filler materials for enhancing biogas separation membranes. *Chem. Rev.* **2018**, *118*, 8655–8769. [CrossRef]
11. Vinh-Thang, H.; Kaliaguine, S. Predictive models for mixed-matrix membrane performance: A review. *Chem. Rev.* **2013**, *113*, 4980–5028. [CrossRef] [PubMed]
12. Aroon, M.; Ismail, A.; Matsuura, T.; Montazer-Rahmati, M. Performance studies of mixed matrix membranes for gas separation: A review. *Sep. Purif. Technol.* **2010**, *75*, 229–242. [CrossRef]

13. Bastani, D.; Esmaeili, N.; Asadollahi, M. Polymeric mixed matrix membranes containing zeolites as a filler for gas separation applications: A review. *J. Ind. Eng. Chem.* **2013**, *19*, 375–393. [CrossRef]
14. Khdhayyer, M.R.; Esposito, E.; Fuoco, A.; Monteleone, M.; Giorno, L.; Jansen, J.C.; Attfield, M.P.; Budd, P.M. Mixed matrix membranes based on UiO-66 MOFs in the polymer of intrinsic microporosity PIM-1. *Sep. Purif. Technol.* **2017**, *173*, 304–313. [CrossRef]
15. Ghalei, B.; Sakurai, K.; Kinoshita, Y.; Wakimoto, K.; Isfahani, A.P.; Song, Q.; Doitomi, K.; Furukawa, S.; Hirao, H.; Kusuda, H.; et al. Enhanced selectivity in mixed matrix membranes for CO_2 capture through efficient dispersion of amine-functionalized MOF nanoparticles. *Nat. Energy* **2017**, *2*, 17086. [CrossRef]
16. Fuoco, A.; Khdhayyer, M.R.; Attfield, M.P.; Esposito, E.; Jansen, J.C.; Budd, P.M. Synthesis and Transport Properties of Novel MOF/PIM-1/MOF Sandwich Membranes for Gas Separation. *Membranes* **2017**, *7*, 7. [CrossRef] [PubMed]
17. Song, Q.; Nataraj, S.; Roussenova, M.V.; Tan, J.C.; Hughes, D.J.; Li, W.; Bourgoin, P.; Alam, M.A.; Cheetham, A.K.; Al-Muhtaseb, S.A.; et al. Zeolitic imidazolate framework (ZIF-8) based polymer nanocomposite membranes for gas separation. *Energy Environ. Sci.* **2012**, *5*, 8359–8369. [CrossRef]
18. Sanchez-Lainez, J.; Zornoza, B.; Friebe, S.; Caro, J.; Cao, S.; Sabetghadam, A.; Seoane, B.; Gascon, J.; Kapteijn, F.; le Guillouzer, C.; et al. Influence of ZIF-8 particle size in the performance of polybenzimidazole mixed matrix membranes for pre-combustion CO_2 capture and its validation through interlaboratory test. *J. Membr. Sci.* **2016**, *515*, 45–53. [CrossRef]
19. Smith, S.J.; Ladewig, B.P.; Hill, A.J.; Lau, C.H.; Hill, M.R. Post-synthetic Ti exchanged UiO-66 metal-organic frameworks that deliver exceptional gas permeability in mixed matrix membranes. *Sci. Rep.* **2015**, *5*, 7823. [CrossRef]
20. Anjum, M.W.; Vermoortele, F.; Khan, A.L.; Bueken, B.; de Vos, D.E.; Vankelecom, I.F. Modulated UiO-66-based mixed-matrix membranes for CO_2 separation. *ACS Appl. Mater. Interfaces* **2015**, *7*, 25193–25201. [CrossRef]
21. Askari, M.; Chung, T.-S. Natural gas purification and olefin/paraffin separation using thermal cross-linkable co-polyimide/ZIF-8 mixed matrix membranes. *J. Membr. Sci.* **2013**, *444*, 173–183. [CrossRef]
22. Wijenayake, S.N.; Panapitiya, N.P.; Versteeg, S.H.; Nguyen, C.N.; Goel, S.; Balkus, K.J., Jr.; Musselman, I.H.; Ferraris, J.P. Surface cross-linking of ZIF-8/polyimide mixed matrix membranes (MMMs) for gas separation. *Ind. Eng. Chem. Res.* **2013**, *52*, 6991–7001. [CrossRef]
23. Pan, Y.; Liu, Y.; Zeng, G.; Zhao, L.; Lai, Z. Rapid synthesis of zeolitic imidazolate framework-8 (ZIF-8) nanocrystals in an aqueous system. *Chem. Commun.* **2011**, *47*, 2071–2073. [CrossRef] [PubMed]
24. Shi, Q.; Chen, Z.; Song, Z.; Li, J.; Dong, J. Synthesis of ZIF-8 and ZIF-67 by Steam-Assisted Conversion and an Investigation of Their Tribological Behaviors. *Angew. Chem.* **2011**, *123*, 698–701. [CrossRef]
25. Katz, M.J.; Brown, Z.J.; Colón, Y.J.; Siu, P.W.; Scheidt, K.A.; Snurr, R.Q.; Hupp, J.T.; Farha, O.K. A facile synthesis of UiO-66, UiO-67 and their derivatives. *Chem. Commun.* **2013**, *49*, 9449–9451. [CrossRef] [PubMed]
26. Kitagawa, S. Metal–organic frameworks (MOFs). *Chem. Soc. Rev.* **2014**, *43*, 5415–5418.
27. Basu, S.; Cano-Odena, A.; Vankelecom, I.F. MOF-containing mixed-matrix membranes for CO_2/CH_4 and CO_2/N2 binary gas mixture separations. *Sep. Purif. Technol.* **2011**, *81*, 31–40. [CrossRef]
28. Fu, Y.-J.; Liao, K.-S.; Hu, C.-C.; Lee, K.-R.; Lai, J.-Y. Development and characterization of micropores in carbon molecular sieve membrane for gas separation. *Microporous Mesoporous Mater.* **2011**, *143*, 78–86. [CrossRef]
29. Zornoza, B.; Tellez, C.; Coronas, J.; Gascon, J.; Kapteijn, F. Metal organic framework based mixed matrix membranes: An increasingly important field of research with a large application potential. *Microporous Mesoporous Mater.* **2013**, *166*, 67–78. [CrossRef]
30. Nijem, N.; Wu, H.; Canepa, P.; Marti, A.; Balkus, K.J., Jr.; Thonhauser, T.; Li, J.; Chabal, Y.J. Tuning the gate opening pressure of metal–organic frameworks (MOFs) for the selective separation of hydrocarbons. *J. Am. Chem. Soc.* **2012**, *134*, 15201–15204. [CrossRef]
31. Wu, H.; Chua, Y.S.; Krungleviciute, V.; Tyagi, M.; Chen, P.; Yildirim, T.; Zhou, W. Unusual and highly tunable missing-linker defects in zirconium metal–organic framework UiO-66 and their important effects on gas adsorption. *J. Am. Chem. Soc.* **2013**, *135*, 10525–10532. [CrossRef] [PubMed]
32. Robeson, L.M. The upper bound revisited. *J. Membr. Sci.* **2008**, *320*, 390–400. [CrossRef]
33. Bromberg, L.; Cohn, D.; Rabinovich, A.; Alexeev, N. Plasma catalytic reforming of methane. *Int. J. Hydrogen Energy* **1999**, *24*, 1131–1137. [CrossRef]

34. Freeman, B.; Yampolskii, Y.; Pinnau, I. *Materials Science of Membranes for Gas and Vapor Separation*; John Wiley & Sons: Hoboken, NJ, USA, 2006.
35. Saberi, M.; Dadkhah, A.; Hashemifard, S. Modeling of simultaneous competitive mixed gas permeation and CO_2 induced plasticization in glassy polymers. *J. Membr. Sci.* **2016**, *499*, 164–171. [CrossRef]